ACS APPLIED ENERGY MATERIALS

www.acsaem.org Article

Elucidating Anisotropic Ionic Diffusion Mechanism in Li_3YCl_6 with Molecular Dynamics Simulations

Jiazhong Geng, Zihan Yan, and Yizhou Zhu*

Cite This: *ACS Appl. Energy Mater.* 2024, 7, 7019−7024 Read Online

ACCESS | Metrics & More | Article Recommendations | Supporting Information

ABSTRACT: Halide-based solid electrolytes have emerged as promising materials for the development of solid-state batteries, due to their high ionic conductivity and excellent chemical properties. Li_3YCl_6 is a prototype halide-based superionic material that features anisotropic ionic diffusion. Elucidating the ionic transport and optimizing the conductivity in such anisotropic materials are crucial for enhancing the performance of solid-state batteries. In this work, by using molecular dynamics simulations with a machine learning force field, we systematically study the anisotropic ion diffusion behavior, including directional conductivity contribution, concerted migration, and disorder−order transition in Li_3YCl_6. Our results prove that the fast *c*-direction is the major contributor to total diffusivity, especially at room temperature. The hexagonal close-packed anion arrangement leads to anisotropic diffusion mechanism. Lithium diffusion along the *c*-direction exhibits a highly concerted feature, which is absent in the *ab*-plane diffusion. A disorder−order transition of the lithium sublattice can occur below a critical temperature. Our results show that the ordering occurs with a regular pattern of lithium ions. The lithium sublattice ordering is strongly influenced by yttrium cation arrangement and can be suppressed if a small amount of Li/Y antisite defects are present. These understandings can help to provide guidance for the future development of anisotropic superionic materials.

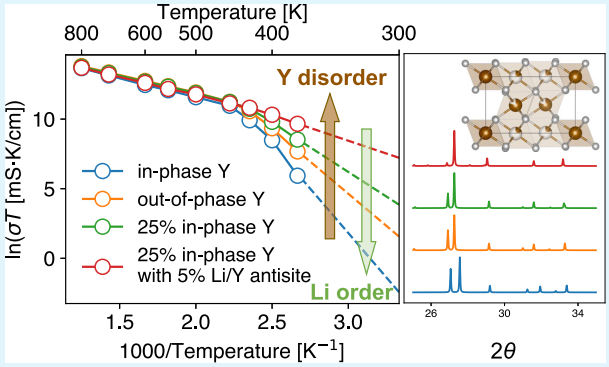

KEYWORDS: *solid electrolyte, solid-state battery, anisotropic diffusion, materials design, molecular dynamics simulation*

Downloaded via WESTLAKE UNIV on November 16, 2024 at 05:58:40 (UTC).
See https://pubs.acs.org/sharingguidelines for options on how to legitimately share published articles.

■ INTRODUCTION

Solid electrolytes with superionic transport are crucial for the development of all-solid-state batteries, which are considered promising next-generation energy storage systems. Thanks to recent advancements, halides have emerged as a new group of promising candidates as solid electrolyte materials.[1] Several halide-based solid electrolytes, such as Li_3InCl_6, Li_3ScCl_6, and $Li_3Y(Br_3Cl_3)$, can achieve ionic conductivities of 1.54−7.2 mS/cm at room temperature,[2−4] surpassing most oxides and rivaling some of the best-performing sulfides.[5] Additionally, halide solid electrolytes exhibit wide electrochemical stability windows, particularly demonstrating much higher anodic limits compared to sulfides.[6] Moreover, halides exhibit significantly better moisture stability than sulfides due to their unique anion chemistry.[7]

Among halide solid electrolytes, Li_3YCl_6 serves as a typical prototype material with a hexagonal close-packed (hcp) arrangement of anions (Figure 1a) and has been studied extensively both experimentally and theoretically. In an hcp-anion framework, lithium ions can migrate either between face-sharing octahedral sites directly (o-o path) along the *c*-direction, or through an intermediate tetrahedral site between edge-sharing octahedral sites (o-t-o path) within the *ab*-plane. Previous studies have shown that ion diffusion along the *c*-direction is usually faster thanks to its lower migration barrier (0.19−0.25 eV) than that within the *ab*-plane (0.29−0.39 eV).[8] Therefore, a halide solid electrolyte with an hcp-anion sublattice generally exhibits anisotropic ionic diffusion.

Besides anion packing, cation arrangement is another crucial factor that dictates the lithium diffusion mechanism.[9−11] Wang et al. used ab initio molecular dynamics (MD) simulations to study the effect of Y/Li antisite defects in Li_3YCl_6, which are also a kind of cation disordering, and concluded that these antisite defects might be detrimental to lithium diffusion due to the channel-blocking effect.[8] Later, they performed MD simulations with a machine learning force field and found that the mobile Li sublattice goes through a superionic transition at 425 K, with a drastic increase of activation energy under lower temperature.[12] By using neutron diffraction, Schlem et al. discovered that different synthesis approaches have a significant effect on yttrium cation disordering, among which

Received: May 15, 2024
Revised: July 23, 2024
Accepted: July 24, 2024
Published: August 2, 2024

© 2024 American Chemical Society

https://doi.org/10.1021/acsaem.4c01249
ACS Appl. Energy Mater. 2024, 7, 7019−7024

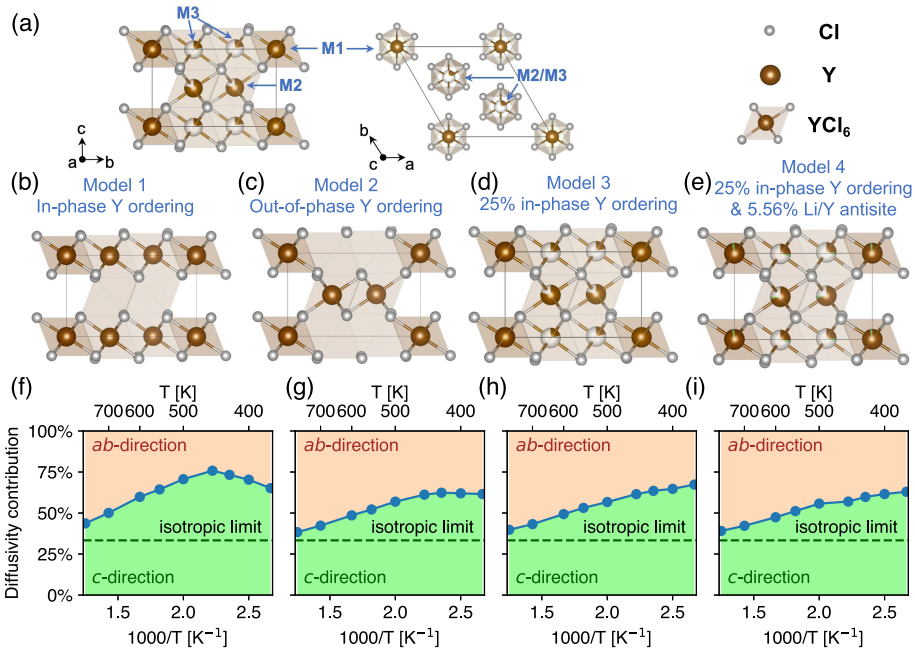

Figure 1. (a) Framework structure of Li_3YCl_6 with three different Y sites, M1, M2, and M3. All lithium ions were omitted. We propose four framework models with (b) in-phase Y ordering, (c) out-of-phase Y ordering, (d) 25% in-phase Y ordering, and (e) 25% in-phase Y ordering with 5.56% Li/Y antisite defects. (f−i) Corresponding directional diffusivity contributions of the four models from 375 to 800 K, in which the orange and green regions represent the contribution from the *ab*-direction and *c*-direction, respectively. The dashed lines refer to the isotropic limit.

ball-milling is the most effective way to promote yttrium disordering and ionic conductivity.[13] Recently, Yu et al. proposed that, for Li_3YCl_6, in-plane diffusion is the rate limiting factor of lithium diffusion. They suggested that compared to in-phase Y ordering where all Y ions arranged in alternating layers (Figure 1b), an out-of-phase Y ordering (Figure 1c) can promote the in-plane lithium-ion diffusion and therefore increase the extrapolated ionic conductivity under room temperature.[11]

Despite previous research efforts, several key challenges in understanding and designing these anisotropic halide superionic materials remain unresolved. First, for anisotropic materials such as Li_3YCl_6, it is crucial to distinguish which direction is the primary contributor to the total ionic conductivity, especially under room temperature. Besides, the disordered arrangement of yttrium cations, resulting from different synthesis approaches, strongly dictates the diffusion of lithium ions. However, such structure−property relationship is still unclear, especially considering the partial occupancy change between different yttrium sites. To the best of our knowledge, all previous first-principles calculations or MD simulations were performed in a relatively small supercell up to 60 atoms, which may be insufficient to capture the effect from yttrium disordering. Lastly, Li/Y antisite defects were considered as detrimental to lithium diffusion.[8] Despite no significant Li/Y antisite defects being experimentally observed,[14] a small amount of such defects could still be introduced by mechanochemical approaches and their effects on lithium diffusion and superionic transition remain elusive.

In this study, we address these challenges by employing molecular dynamics simulations in Li_3YCl_6 with a machine learning force field (MLMD) in a large supercell containing 2160 atoms. In contrast to previous work,[11] we demonstrate that regardless of the cation arrangement, the *c*-direction consistently emerges as the primary contributor to total ionic conductivity, particularly at lower temperatures. Additionally, we identify a highly anisotropic diffusion mechanism in Li_3YCl_6. While diffusion within the *ab*-plane remains mostly nonconcerted, lithium ions exhibit highly concerted migration along the *c*-direction. The degree of concerted migration is influenced by the temperature and cation arrangement. Moreover, we reveal that the disorder−order transition of Li_3YCl_6 occurs through lithium sublattice ordering, discernible through both the probability distribution of spatial occupancy and the presence of a superstructure peak in virtual X-ray diffraction (XRD) patterns. Different Y cation ordering leads to different degrees of lithium sublattice ordering below the transition temperature, which we believe is the major reason why different synthesis approaches affect the ionic diffusivity. Lastly, we reveal that Li/Y antisite defects, previously suspected to be detrimental to ion diffusion, can suppress the disorder−order transition and maintain the disordered lithium sublattice under low temperature. We discuss the potential engineering strategies for the future optimization and design of anisotropic halide superionic materials.

■ RESULTS AND DISCUSSION

Li_3YCl_6 with $P\bar{3}m1$ space group contains three types of Y sites, including a fully occupied 1*a* positions M1 and two partially occupied 2*d* positions M2 and M3 in (002) and (001) planes, respectively (Figure 1a).[15,16] Here we adopt the notation from previous studies.[13,17] The M2 and M3 sites exhibit different degrees of disorder due to various synthesis conditions. Experimentally, the M3 site is usually more occupied (∼77%) than the M2 site (∼23%).[18] We construct four representative structures with different Y ordering. Model 1 refers to in-phase Y ordering, in which M1 and M3 are fully occupied with a vacant M2 site; therefore, all Y ions are arranged in alternating layers (Figure 1b). Model 2 refers to out-of-phase Y ordering where only M1 and M2 sites are fully

https://doi.org/10.1021/acsaem.4c01249
ACS Appl. Energy Mater. 2024, 7, 7019−7024

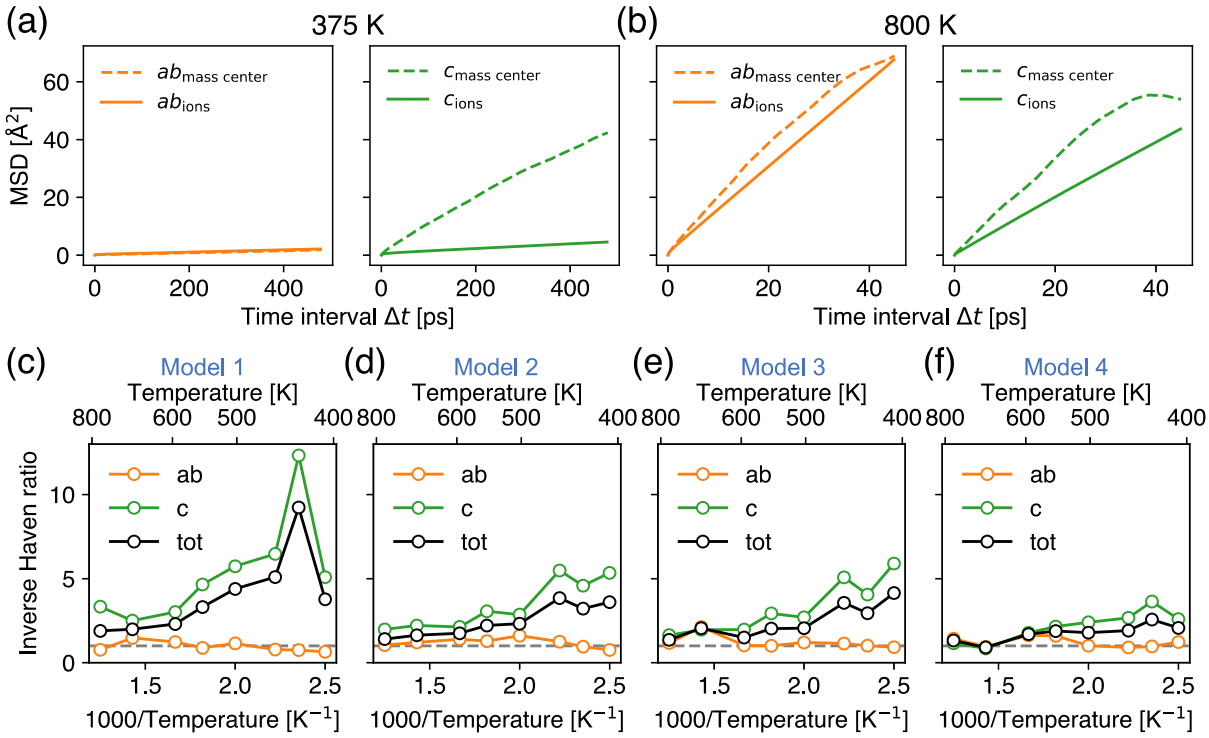

Figure 2. Dimensional mean squared displacements (MSDs) from MD simulations of lithium ions (solid lines) and their center of mass (dashed lines) at (a) 375 and (b) 800 K. Data from MD simulations based on Model 3 (25% in-phase Y ordering). The MSD of lithium center of mass is multiplied by the number of lithium atoms for comparison. (c−f) Total and directional inverse Haven ratio of four models with different Y orderings. The dashed horizontal line refers to when no concerted migration is activated, and Haven ratio equals one.

occupied, so M1 pillars along the *c*-direction always have the opposite occupancy with its neighboring M2/M3 pillars (Figure 1c). Model 3 is closer to the experimentally characterized structure from solid-state synthesized samples, in which 25% and 75% Y occupies M3 and M2 sites, respectively (Figure 1d). Model 4 aims to study the effect from Li/Y antisite defects,[8] which is based on Model 3 but with additional 5.56% Li/Y antisites defects (Figure 1e).

Dominating Ion Diffusion Direction in Anisotropic Diffusion. We first elucidate which direction (*ab*-direction or *c*-direction) dominates ion diffusion under different temperatures, since anisotropic diffusion is a key feature of Li_3YCl_6. We quantify the anisotropy of ion diffusion by the contribution from the directional diffusivity to the overall diffusivity. The isotropic limit refers to when the *c*-direction contributes one-third to the total diffusivity. Contrary to previous reports,[11] our results show that, for all four models, the contribution from the *c*-direction is consistently higher than the isotropic limit (Figure 1f−i). At 800 K, the contribution from the *c*-direction is around 40%, while at 375 K, the *c*-direction contribution exceeds 60%, indicating that the fast *c*-direction should be the major contributor to total diffusivity under room temperature.

The anisotropic nature of fast ion diffusion in Li_3YCl_6 motivates us to investigate if concerted migrations are present, since it is a characteristic feature of multiple oxide-based and sulfide-based superionic materials.[19] We calculate the mean squared displacements (MSDs) of lithium ions as well as the MSDs of their centers of mass in different directions, from which the tracer and conductivity diffusivities (D_{tr} and D_{σ}) can be extracted from the slope, respectively. Here we used Model 3 (25% in-phase Y ordering) as our model system (data for other models are available in Supporting Information Figures S2−S4). At 800 K, diffusion in the *ab*-plane is mostly nonconcerted, while that in the *c*-direction shows a slightly concerted migration feature (Figure 2b). However, as the temperature drops to 375 K, diffusion within the *ab*-plane remains nonconcerted, while diffusion along the *c*-direction becomes highly concerted, as the MSD of the mass center is about 4 times higher than that of ions. (Figure 2a). Such a difference indicates that the in-plane diffusion maintains a nonconcerted single-ion hopping mode under different temperatures, while the *c*-direction diffusion exhibits a from weak to strong concerted migration mode as the temperature decreases from 800 to 375 K.

The inverse Haven ratio (D_{σ}/D_{tr}) quantifies the degree of concerted migration (Figure 2c,f). For all four models, diffusion within the *ab*-plane remains nonconcerted and is essentially unaffected by temperature. In contrast, the *c*-direction diffusion always exhibits a certain degree of concerted migration under all temperatures. When temperature is at 500−700 K, the inverse Haven ratio is around 2−3. Note that such a degree of concerted migration is already comparable to that in some of the well-known superionic materials with concerted migration mode, such as $Li_{10}GeP_2S_{12}$ (3.0), cubic lithium garnet $Li_7La_3Zr_2O_{12}$ (3.0), and $Li_{1.3}Al_{0.3}Ti_{1.7}(PO_4)_3$ (2.1).[19] As the temperature decreases to below 500 K, the concerted migration mode is further enhanced. Model 1 with in-phase Y ordering shows the strongest concerted migration mode, with inverse Haven ratio exceeding 5 (Figure 2c). Model 2 with out-of-phase Y ordering and Model 3 with 25% in-phase Y ordering show similar behaviors with Haven ratios close to 5 (Figure 2d,e). Model 4 containing Li/Y antisite defects shows the mildest increase of inverse Haven ratio, reaching around 3 at low temperatures. By examining a

https://doi.org/10.1021/acsaem.4c01249
ACS Appl. Energy Mater. 2024, 7, 7019−7024

trajectory movie obtained from MD simulations under low temperature (Model 3, 375 K, Supporting Information Movie S1), concerted migration modes can be visualized. The Li ions occupying octahedral sites experience strong Coulomb repulsion interactions from nearby lithium ions within a distance of about 3 Å. Such strong Coulomb interactions can result in concerted migration modes with lower migration barriers, similar to the behavior of Li ions in LLZO and LATP.[19]

Our finding contradicts a previous report, which claims the absence of notable concerted migration in Li_3YCl_6.[8] Despite no concerted migration in the *ab*-plane observed in Li_3YCl_6, very strong concerted migrations are observed in ion diffusion along the fast *c*-direction, further highlighting its anisotropic nature.

Disorder−Order Transition in Lithium Sublattice. A disorder−order transition can occur in Li_3YCl_6 when the temperature drops below $T_c \sim 425$ K, as reported in previous studies.[12,20] This phase transition is accompanied by an abrupt increase in the activation energy E_a. However, a relationship between the phase transition and the Y cation ordering has not been established. Our MLMD results show that all four models exhibit similar diffusivities and a common E_a of 0.23 eV when the temperature is above 450 K. Nevertheless, different behaviors were observed as the temperature decreases to below 450 K. For our first three models containing a different degree of Y ordering but no Li/Y antisite defects, the phase transition occurs roughly at the same T_c around 425−450 K based on the Arrhenius plot (Figure 3). Low-temperature E_a,

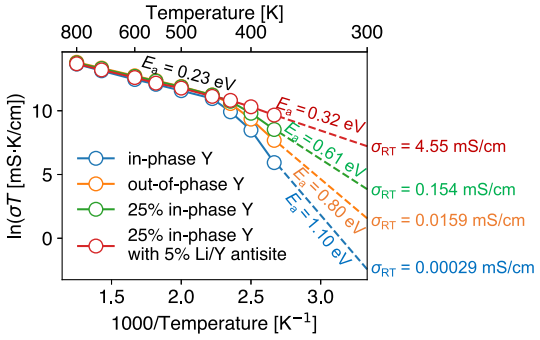

Figure 3. Arrhenius plots of lithium ionic conductivity in four models with different Y orderings. All four models share a common E_a 0.23 eV at high temperatures (≥450 K), while they exhibit different E_a under low temperatures (≤425 K). The room-temperature conductivities σ_{RT} are calculated based on linear extrapolation of low-temperature data to 300 K (dashed lines).

linear fitted from the diffusivity between 375 and 425 K, increase to 1.10, 0.80, and 0.61 eV for in-phase, out-of-phase, and 25% in-phase Y ordering models, respectively. Note that our out-of-phase model has the same Y ordering as in a previous study, which yields a similar low-temperature E_a of 0.74 eV.[12] In contrast, in Model 4 containing 5.56% Li/Y antisite defects, no noticeable sign of a phase transition was observed in the Arrhenius plot across the temperature range we investigated. The low-temperature E_a shows only a slight increase to 0.32 eV.

An important observation is that Model 3, which might be considered as a 25/75 (%) mixture of the in-phase and out-of-phase Y ordering, exhibits a higher ionic conductivity and lower activation energy under low temperature compared to fully in-phase or out-of-phase Y ordering models. This indicates that the effect of Y disordering can be revealed only at a larger length scale. To the best of our knowledge, all previous first-principles calculations or molecular dynamics simulations on Li_3YCl_6 adopt a 1 × 1 × 2 supercell containing 60 atoms, which can only accommodate fully in-phase and out-of-phase Y ordering.[6,8,12,14,20] Our MLMD simulations are the first to adopt a large supercell with up to 2160 atoms, where we can introduce a partially disordered Y sublattice that is closer to the experimentally characterized structure. Our calculated E_a is 0.61 eV and extrapolated room-temperature conductivity σ_{RT} is 0.16 mS/cm, both of which agree well with experiments.[13,21] In contrast, the calculated E_a values for the in-phase and out-of-phase models are 1.10 and 0.80 eV, respectively. And their extrapolated conductivities σ_{RT} are merely 0.00029 and 0.016 mS/cm, respectively. The disordering in the Y-sublattice, which can be promoted through the ball-milling procedure, benefits the ion diffusion below the transition temperature.

Our results show that antisite defects are beneficial to ion diffusion in Li_3YCl_6, as they effectively suppress the undesired phase transition. This is contrary to the previous hypothesis that antisite defects might be detrimental to ion diffusion due to channel-blocking effect.[8] With 5.56% antisite defects, the calculated low-temperature E_a decreases to 0.32 eV, while the extrapolated σ_{RT} reaches 4.55 mS/cm. Despite the absence of experimental evidence of significant Li/Y antisite defects,[14] we suspect that the ball-milling process might introduce a small amount of such defects; therefore, the ball-milled sample generally exhibits better ionic conductivity.[13]

To reveal the underlying structural feature of the disorder−order transition, we calculate the spatial probability density distribution of lithium ions for all four models at 375 K. The first two models with in-phase and out-of-phase Y ordering show similar behaviors, in which lithium orders along the *c*-direction with a regular 3Li-1□ pattern (Figure 4a,b). The 25% in-phase Y ordering model also follows the same pattern, but to a weaker extent, as the occupancy difference between the lithium site and the vacant site becomes smaller (Figure 4c). In addition, this 3Li-1□ pattern also agrees with a

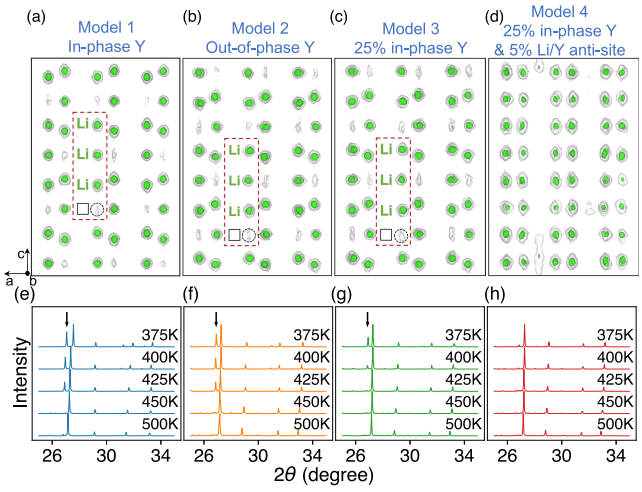

Figure 4. (a−d) Probability density of Li-ion spatial occupancy in four models with different Y orderings from MLMD simulations at 375 K. The inner (green) isosurface density is 6 times that of the outer (gray) isosurface density. (e, h) Simulated virtual XRD patterns (wavelength, 1.542 Å) from all lithium ions in the four models from 375 to 500 K. The superstructure peaks are marked by arrows.

https://doi.org/10.1021/acsaem.4c01249
ACS Appl. Energy Mater. 2024, 7, 7019−7024

previous experimental observation that the Wyckoff 6g and 6h Li sites are roughly equally occupied.[14] When 5.56% Li/Y antisite defects are introduced, the lithium sublattice ordering disappears (Figure 4d), indicating that all available lithium sites exhibit similar occupancy. We propose that those antisite defects disrupt the ordering tendency of a 3Li-1□ pattern and thus effectively suppress the formation of an ordered lithium sublattice. The disordered lithium sublattice has a uniform occupancy distribution among all available lithium sites and therefore activates the frustration mechanism with enhanced lithium diffusion.

Another way to visualize the ordering of the lithium sublattice is through the virtual X-ray diffraction (XRD) patterns. The superstructure reflections, forbidden in a disordered lithium sublattice, arise only when long-range order becomes present. A superstructure peak at 27° relates to the 3Li-1□ lithium sublattice ordering. The appearing temperature of this superstructure peak for the first two models is around 425 K (Figure 4e,f), which agrees with the transition temperature observed in Arrhenius plot. Besides, the relative intensity of the superstructure peak directly correlates with the degree of lithium sublattice ordering. The intensity of the superstructure peak increases as the temperature decreases, and it is weaker for the partially disordered Y-sublattice structure compared to the structure with in-phase or out-of-phase ordered Y-sublattice (Figure 4g). The superstructure peak is almost completely suppressed for the last model containing antisite defects, coinciding with our observation in Arrhenius plot and lithium density spatial distribution (Figure 4h). In addition, the intensity of the superstructure peak decreases when the antisite defect concentration increases (Figure S7). And this approach enables rapid evaluation of the critical concentration of antisite defects needed to suppress the lithium sublattice ordering, which only requires a short time molecular dynamics simulation.

■ CONCLUSION

In summary, by investigating solid electrolyte Li_3YCl_6 with an hcp anion sublattice, we systematically study its anisotropic ion diffusion behavior, including directional conductivity contribution, concerted migration, disorder−order transition, and effect on conductivity. We constructed four Li_3YCl_6 structural models with different Y cation arrangements and Li/Y antisite defects. Our MLMD simulations prove that the fast *c*-direction is the major contributor to total diffusivity, especially under room temperature. The anisotropic hcp-anion framework in Li_3YCl_6 leads to an anisotropic diffusion property and mechanism. Lithium diffusion along the *c*-direction exhibits a highly concerted feature, which is absent in the *ab*-plane diffusion. A disorder−order transition of the lithium sublattice can occur below T_c, accompanied by an increase in E_a and a decrease in diffusivity. We find that the formed ordering follows a 3Li-1□ pattern along the *c*-direction, as observed in the spatial density distribution of lithium ions. The ordering is also reflected by a superstructure peak in the virtual XRD patterns. The lithium sublattice ordering behavior is influenced by the arrangement of Y cations and can be suppressed if small amounts of Li/Y antisite defects are present.

Our understanding can provide a practical engineering strategy for optimizing anisotropic halide solid electrolyte materials. Optimizing ion diffusion in the *c*-direction, which is the main conductivity contributing direction, is an effective strategy for improving the ion conductivity of Li_3YCl_6, particularly at room temperature. Suppression of the undesired disorder−order transition is the key to improving the room-temperature ionic conductivity in Li_3YCl_6, and we believe such a strategy might be generally applicable for other anisotropic halide-based solid electrolyte materials with an hcp anion framework. Introducing Li/Y antisite defects in the lattice has been confirmed as beneficial to suppress undesired disorder−order transition and to enhance low-temperature ion diffusion. This explains the differences in the performance of Li_3YCl_6 synthesized under different experimental conditions. Other potential strategies include aliovalent doping and lithium stoichiometry change, which can lead to frustration in lithium sublattice to break the ordering tendency.[10,12] Our research reveals the ion diffusion characteristics in anisotropic materials and provides practical engineering strategies to further optimize the ion conductivity of the material at room temperature, thereby providing guidance for designing high-performance solid-state electrolyte materials.

■ COMPUTATIONAL METHODS

A machine-learning force field (MLFF) using the Deep Potential (DP) formalism[22] is trained through the active learning scheme implemented in the DP-GEN package.[23] The trained MLFF accurately reproduces the energies and forces in agreement with density functional theory (DFT) calculations (Figure S1). Exploration iterations in DP-GEN are shown in Table S1.

Molecular dynamics (MD) simulations and XRD simulated patterns were performed with the LAMMPS package.[24] We constructed orthogonal supercells containing 2160 atoms, 648 of which are lithium atoms. The lattice vectors of the supercell a_s, b_s, and c_s are $a_s = 3a_0$, $b_s = 2a_0 + 4b_0$, and $c_s = 6c_0$, where a_0, b_0, and c_0 are the lattice vectors of the unit cell. The initial structures were heated in *NPT* ensembles at standard atmospheric pressure to the desired temperature (375−800 K) over 30 ps and then equilibrated at the equilibrium temperature for 60 ps to acquire averaged lattice parameter under given temperature. Simulation with *NVT* ensembles for quantifying ion diffusion were then performed using the acquired lattice parameter. The MLMD simulation time was set to 0.5 ns when temperatures are above or equal to 500 K. And the simulation times were extended to 1, 2, 10, and 15 ns when the temperatures were 450, 425, 400, and 375 K, respectively. For all simulations, time steps were set to 1 fs.

■ ASSOCIATED CONTENT

Supporting Information

The Supporting Information is available free of charge at https://pubs.acs.org/doi/10.1021/acsaem.4c01249.

Movie S1 showing trajectory concerted migration (MP4)

Machine-learning interatomic potential model training; ion diffusion data and calculation methods; discussions on anisotropic diffusion; simulated sublattice XRD patterns (PDF)

■ AUTHOR INFORMATION

Corresponding Author

Yizhou Zhu − *School of Engineering and Research Center for Industries of the Future, Westlake University, Hangzhou, Zhejiang 310030, China*; orcid.org/0000-0002-5819-7657; Email: zhuyizhou@westlake.edu.cn

Authors

Jiazhong Geng − *School of Engineering, Westlake University, Hangzhou, Zhejiang 310030, China*

https://doi.org/10.1021/acsaem.4c01249
ACS Appl. Energy Mater. 2024, 7, 7019−7024

Zihan Yan − *School of Engineering, Westlake University, Hangzhou, Zhejiang 310030, China;* orcid.org/0000-0002-8911-6549

Complete contact information is available at: https://pubs.acs.org/10.1021/acsaem.4c01249

Notes

The authors declare no competing financial interest.

■ ACKNOWLEDGMENTS

We acknowledge the support from the Research Center for Industries of the Future (RCIF) and the High-Performance Computing Center (HPC) at Westlake University.

■ REFERENCES

(1) Li, X.; Kim, J. T.; Luo, J.; Zhao, C.; Xu, Y.; Mei, T.; Li, R.; Liang, J.; Sun, X. Structural regulation of halide superionic conductors for all-solid-state lithium batteries. *Nat. Commun.* **2024**, *15*, 53.

(2) Liu, Z.; Ma, S.; Liu, J.; Xiong, S.; Ma, Y.; Chen, H. High ionic conductivity achieved in $Li_3Y(Br_3Cl_3)$ mixed halide solid electrolyte via promoted diffusion pathways and enhanced grain boundary. *ACS Energy Lett.* **2021**, *6*, 298−304.

(3) Li, X.; Liang, J.; Chen, N.; Luo, J.; Adair, K. R.; Wang, C.; Banis, M. N.; Sham, T. K.; Zhang, L.; Zhao, S.; Lu, S.; Huang, H.; Li, R.; Sun, X. Water-mediated synthesis of a superionic halide solid electrolyte. *Angew. Chem., Int. Ed.* **2019**, *131*, 16579−16584.

(4) Liang, J.; Li, X.; Wang, S.; Adair, K. R.; Li, W.; Zhao, Y.; Wang, C.; Hu, Y.; Zhang, L.; Zhao, S.; Lu, S.; Huang, H.; Li, R.; Mo, Y.; Sun, X. Site-occupation-tuned superionic Li_xScCl_{3+x} halide solid electrolytes for all-solid-state batteries. *J. Am. Chem. Soc.* **2020**, *142*, 7012−7022.

(5) Nikodimos, Y.; Su, W. N.; Hwang, B. J. Halide solid-state electrolytes: stability and application for high voltage all-solid-state Li batteries. *Adv. Energy Mater.* **2023**, *13*, No. 2202854.

(6) Li, X.; Liang, J.; Yang, X.; Adair, K. R.; Wang, C.; Zhao, F.; Sun, X. Progress and perspectives on halide lithium conductors for all-solid-state lithium batteries. *Energy Environ. Sci.* **2020**, *13*, 1429.

(7) Zhu, Y.; Mo, Y. Materials design principles for air-stable lithium/sodium solid electrolytes. *Angew. Chem., Int. Ed.* **2020**, *59*, 17472−17476.

(8) Wang, S.; Bai, Q.; Nolan, A. M.; Liu, Y.; Gong, S.; Sun, Q.; Mo, Y. Lithium chlorides and bromides as promising solid-state chemistries for fast ion conductors with good electrochemical stability. *Angew. Chem., Int. Ed.* **2019**, *58*, 8039−8043.

(9) Liu, Y.; Wang, S.; Nolan, A. M.; Ling, C.; Mo, Y. Tailoring the cation lattice for chloride lithium-ion conductors. *Adv. Energy Mater.* **2020**, *10*, No. 2002356.

(10) Zhong, P.; Gupta, S.; Deng, B.; Jun, K. J.; Ceder, G. The effect of cation-disorder on lithium transport in halide superionic conductors. *ACS Energy Lett.* **2024**, *9*, (6), 2775−2781.

(11) Yu, S.; Noh, J.; Kim, B.; Song, J. H.; Oh, K.; Yoo, J.; Lee, S.; Park, S. O.; Kim, W.; Kang, B.; Kil, D.; Kang, K. Design of a trigonal halide superionic conductor by regulating cation order-disorder. *Science* **2023**, *382*, 573−579.

(12) Wang, S.; Liu, Y.; Mo, Y. Frustration in super-ionic conductors unraveled by the density of atomistic states. *Angew. Chem., Int. Ed.* **2023**, *62*, No. e202215544.

(13) Schlem, R.; Muy, S.; Prinz, N.; Banik, A.; Shao-Horn, Y.; Zobel, M.; Zeier, W. G. Mechanochemical synthesis: a tool to tune cation site disorder and ionic transport properties of Li_3MCl_6 (M = Y, Er) superionic conductors. *Adv. Energy Mater.* **2020**, *10*, No. 1903719.

(14) Schlem, R.; Banik, A.; Ohno, S.; Suard, E.; Zeier, W. G. Insights into the lithium sub-structure of superionic conductors Li_3YCl_6 and Li_3YBr_6. *Chem. Mater.* **2021**, *33*, 327−337.

(15) Asano, T.; Sakai, A.; Ouchi, S.; Sakaida, M.; Miyazaki, A.; Hasegawa, S. Solid halide electrolytes with high lithium-ion conductivity for application in 4 V class bulk-type all-solid-state batteries. *Adv. Mater.* **2018**, *30*, No. 1803075.

(16) Ahammed, B.; Ertekin, E. Configurational disorder, strong anharmonicity, and coupled host dynamics lead to superionic transport in Li_3YCl_6 (LYC). *Adv. Mater.* **2024**, *36*, No. 2310537.

(17) Sebti, E.; Evans, H. A.; Chen, H.; Richardson, P. M.; White, K. M.; Giovine, R.; Koirala, K. P.; Xu, Y.; Gonzalez-Correa, E.; Wang, C.; Brown, C. M.; Cheetham, A. K.; Canepa, P.; Clément, R. J. Stacking faults assist lithium-ion conduction in a halide-based superionic conductor. *J. Am. Chem. Soc.* **2022**, *144*, 5795−5811.

(18) van der Maas, E.; Famprikis, T.; Pieters, S.; Dijkstra, J. P.; Li, Z.; Parnell, S. R.; Smith, R. I.; van Eck, E. R. H.; Ganapathy, S.; Wagemaker, M. Re-investigating the structure−property relationship of the solid electrolytes $Li_{3-x}In_{1-x}Zr_xCl_6$ and the impact of In−Zr(IV) Substitution. *J. Mater. Chem. A* **2023**, *11*, 4559−4571.

(19) He, X.; Zhu, Y.; Mo, Y. Origin of fast ion diffusion in superionic conductors. *Nat. Commun.* **2017**, *8*, No. 15893.

(20) Qi, J.; Banerjee, S.; Zuo, Y.; Chen, C.; Zhu, Z.; Holekevi Chandrappa, M.L.; Li, X.; Ong, S.P. Bridging the gap between simulated and experimental ionic conductivities in lithium superionic conductors. *Mater. Today Phys.* **2021**, *21*, No. 100463.

(21) Zhou, L.; Zuo, T. T.; Kwok, C. Y.; Kim, S. Y.; Assoud, A.; Zhang, Q.; Janek, J.; Nazar, L. F. High areal capacity, long cycle life 4 V ceramic all-solid-state Li-ion batteries enabled by chloride solid electrolytes. *Nat. Energy.* **2022**, *7*, 83−93.

(22) Zhang, L.; Han, J.; Wang, H.; Car, R.; E, W. Deep potential molecular dynamics: a scalable model with the accuracy of quantum mechanics. *Phys. Rev. Lett.* **2018**, *120*, No. 143001.

(23) Zhang, Y.; Wang, H.; Chen, W.; Zeng, J.; Zhang, L.; Wang, H.; E, W. DP-GEN: A concurrent learning platform for the generation of reliable deep learning based potential energy models. *Comput. Phys. Commun.* **2020**, *253*, No. 107206.

(24) Plimpton, S. Fast parallel algorithms for short-range molecular dynamics. *J. Comput. Phys.* **1995**, *117*, 1.